R-symmetry breaking and O'Raifeartaigh model with global symmetries at finite temperature

Masato Arai,[1,*] Yoshishige Kobayashi,[2,†] and Shin Sasaki[2,‡]

[1]*Institute of Experimental and Applied Physics, Czech Technical University in Prague,*
Horská 3a/22, 128 00 Prague 2, Czech Republic
[2]*Department of Physics, Tokyo Institute of Technology, Tokyo 152-8551, Japan*

We investigate finite temperature effects in O'Raifeartaigh models with global symmetries which exhibit supersymmetry breaking at a metastable vacuum accompanied by $U(1)_R$ breaking. The pseudo-moduli field is stabilized at one-loop order at zero temperature within some coupling parameter region. We analyze the behavior of the parameter space according to nonzero temperatures and find that the parameter region which allows $U(1)_R$ breaking is considerably extended at sufficiently low temperature, even though it shrinks down at high temperature as expected. We also discuss the thermal history of the metastable supersymmetry breaking vacuum.

PACS numbers: 12.60.Jv, 11.10.Wx

I. INTRODUCTION

No one doubts that supersymmetry breaking has been the long-standing problem in high energy particle physics and the problem is closely related to the existence of global *R* symmetry. The relation between supersymmetry breaking and global *R* symmetry has been studied after its connection was established in [1]. The authors of [1] showed that in order to break supersymmetry at a global minimum of the potential in generic models, there must exist global $U(1)_R$ symmetry. However, the $U(1)_R$ symmetry should be broken at the supersymmetry breaking vacua, otherwise gauginos cannot have nonzero masses that are phenomenologically required.

A possible solution to this puzzle is to consider a local but not global minimum of the potential to break supersymmetry. In [2], Intriligator, Seiberg, and Shih studied a low-energy effective potential of an $\mathcal{N} = 1$ supersymmetric QCD (ISS model) which exhibits supersymmetry breaking at a local vacuum. This vacuum is metastable but can be long lived, compared to the lifetime of the Universe.

Other models with supersymmetry breaking at local vacua have been studied. It has been shown that O'Raifeartaigh models [3] with fields that have *R* charges different from 0 or 2 can have a metastable supersymmetry breaking vacuum without $U(1)_R$ symmetry [4]. In these models, supersymmetry is broken at tree level while the $U(1)_R$ symmetry is broken at one-loop order. Models with tree-level *R*-symmetry breaking were investigated in [5].

It is useful to generalize these models to ones with global symmetries [6]. Such an extension is important since if global symmetries are gauged as gauge groups of the standard model, supersymmetry breaking is mediated to the visible sector through direct gauge mediation mechanisms.[1] These observations open up more possibilities for constructing phenomenologically viable models (for example, see [8]) and the realization of long-lived local vacua in field theories provides a good example to study the string landscape problem [9].

It is also interesting to study the thermal effects of these local vacua. The thermal effects generically modify the structure of the vacua and change the view of the landscape. Since we believe that supersymmetry is broken at the early universe after inflation, it is useful to analyze the thermal history of the hidden sector. The thermal history of supersymmetric models with supersymmetry breaking has been investigated in the context of the ISS model [10–13] and the O'Raifeartaigh-type model without $U(1)_R$ symmetry [14]. The thermal effects of a broad class of models of gauge mediation were also considered [15].

In this paper we study effects of finite temperature on the O'Raifeartaigh-type model with global symmetry considered in [6]. Classically this model has a flat direction of local extrema and a supersymmetric runaway vacuum. One-loop corrections stabilize the flat direction, leading to a spontaneous $U(1)_R$ breaking vacuum in some regions of parameters in the theory. We take account of finite temperature effects and show that such parameter regions shrink down as temperature increases. We also show that parameter regions which are not allowed at zero temperature cause $U(1)_R$ breaking at low temperature. We also address the finite temperature effects along the runaway direction and discuss the thermal evolution of a local vacuum.

---

*masato.arai@utef.cvut.cz
†yosh@th.phys.titech.ac.jp
‡shin-s@th.phys.titech.ac.jp

[1]However, the ISS model and models as in [6] lead to suppressed gaugino mass which is phenomenologically unacceptable [5]. Deformed ISS models have been considered in, for instance, [7].

The organization of this paper is as follows. In the next section, we introduce the model and discuss the supersymmetry breaking vacuum and the runaway direction at zero temperature. In Sec. III, we study finite temperature effects of the model. Especially we investigate behavior of the parameter region according to temperatures. In Sec. IV, we discuss the thermal history of the local vacuum focusing on a specific path to the runaway direction. Section V is the conclusion and discussions. In Appendix A, analytic expressions of the effective potential in high- and low-temperature expansions are shown. In Appendix B, we give explicit expressions of general mass matrices.

II. THE MODEL AND SUPERSYMMETRY BREAKING

In this section, we provide a brief overview of the generalized O'Raifeartaigh model that exhibits supersymmetry breaking without $U(1)_R$ symmetry [4]. We then introduce the model with global symmetry and show the result obtained in [6] at zero temperature.

Consider O'Raifeartaigh models with the following superpotential:

$$W = fX + \tfrac{1}{2}(M^{ij} + XN^{ij})\Phi^i\Phi^j, \qquad (1)$$

$$\det M \neq 0, \qquad \det(M + XN) \neq 0, \qquad (2)$$

where M, N are complex symmetric matrices, f is a real parameter, and X, Φ^i are $\mathcal{N} = 1$ chiral superfields. We assume that the Kähler potential for Φ^i, X is canonical. The condition of $U(1)_R$ charge for each field is $R(X) = 2$ and the other fields satisfy

$$R(\Phi^i) + R(\Phi^j) = 2 \quad \text{for } M^{ij} \neq 0,$$
$$R(\Phi^i) + R(\Phi^j) = 0 \quad \text{for } N^{ij} \neq 0. \qquad (3)$$

The supersymmetric vacuum conditions are given by

$$0 = f + \tfrac{1}{2}N^{ij}\phi^i\phi^j, \qquad 0 = (M^{ij} + N^{ij}X)\phi^j. \qquad (4)$$

Here ϕ^i and X are the lowest component of the superfields Φ^i and X. Because of the condition (2), the equations in (4) cannot be solved simultaneously and the model breaks supersymmetry at an extremum of the potential:

$$\phi^i = 0, \qquad X: \text{arbitrary}. \qquad (5)$$

This solution leaves a flat direction for the X field, which is called pseudomodulus. In order that this extremum is a local vacuum, tachyonic directions must not exist. The bosonic and fermionic mass matrices at this extremum are given by

$$m_B^2 = \begin{pmatrix} (M^\dagger + \bar{X}N^\dagger)(M + XN) & fN^\dagger \\ fN & (M + XN)(M^\dagger\bar{X} + N^\dagger) \end{pmatrix}, \qquad (6)$$

$$m_F^2 = \begin{pmatrix} (M^\dagger + \bar{X}N^\dagger)(M + XN) & 0 \\ 0 & (M + XN)(M^\dagger\bar{X} + N^\dagger) \end{pmatrix}. \qquad (7)$$

If $f = 0$, the Eq. (5) becomes a supersymmetric global vacuum. In this case, all the ϕ directions are not tachyonic and the eigenvalues of $m_B^2 = m_F^2$ are positive. On the other hand, once we turn on $f \neq 0$ terms in the off-diagonal parts in m_B^2, these terms can be considered as perturbations to the positive definite diagonal parts. If the off-diagonal parts are smaller than the diagonal parts, the eigenvalues of m_B^2 can stay in their positive values. Especially if we focus on the small X region, the condition that there are no tachyonic directions is given by $|fN| \ll |M|^2$ which was employed in [6]. In addition to a local supersymmetry breaking minimum, in general, there is also a supersymmetric vacuum in a runaway direction. The local minimum is thus a metastable vacuum.

Since the fields ϕ^i have mass $m^{ij} \sim M^{ij} + XN^{ij}$ at the origin of ϕ^i, given the energy scale lower than this mass, ϕ^i are integrated out and the effective potential for X is obtained. The one-loop effective potential of the pseudomodulus X is given by the Coleman-Weinberg potential [16]

$$V_{\text{eff}}^{\text{CW}}(X) = \frac{1}{64\pi^2}\,\text{Tr}\left[m_B^4\log\frac{m_B^2}{\Lambda^2} - m_F^4\log\frac{m_F^2}{\Lambda^2}\right], \qquad (8)$$

where m_B, m_F are bosonic and fermionic mass matrices and Λ is the dynamical cutoff scale. The total effective potential $V_{\text{eff}}(X)$ is just the sum of V_{tree} and $V_{\text{eff}}^{\text{CW}}$, where V_{tree} is the tree-level potential. The one-loop effective potential generically fixes the modulus X.

It was shown that the model (1) can dynamically break the $U(1)_R$ symmetry at the supersymmetry breaking vacuum by the one-loop corrections if there is a field that has R charge different from 0 or 2 [4]. Once the parameters M, N, and f are chosen appropriately, the pseudomodulus X is stabilized at $X \neq 0$ giving a $U(1)_R$ breaking vacuum as X has nonzero R charge.

The model (1) has been generalized to ones with global symmetry and with more pseudomoduli [6]. In this paper, we focus on the simplest model that has global symmetry

$U(N)$ and one modulus X which is discussed in [6]. The interaction matrices are given by

$$M = \begin{pmatrix} 0 & 0 & 0 & M_5 & 0 & 0 \\ 0 & 0 & 0 & 0 & M_7 & 0 \\ 0 & 0 & 0 & 0 & 0 & M_3 \\ M_5 & 0 & 0 & 0 & 0 & 0 \\ 0 & M_7 & 0 & 0 & 0 & 0 \\ 0 & 0 & M_3 & 0 & 0 & 0 \end{pmatrix},$$

(9)

$$N = \begin{pmatrix} 0 & N_5 & 0 & 0 & 0 & 0 \\ N_5 & 0 & 0 & 0 & 0 & 0 \\ 0 & 0 & 0 & N_3 & 0 & 0 \\ 0 & 0 & N_3 & 0 & 0 & 0 \\ 0 & 0 & 0 & 0 & 0 & 0 \\ 0 & 0 & 0 & 0 & 0 & 0 \end{pmatrix}.$$

The superpotential is given by

$$\begin{aligned} W &= fX + XN_5\phi_{(5)}^a\phi_{(-5)a} + XN_3\phi_{(3)}^a\phi_{(-3)a} \\ &\quad + M_7\phi_{(7)}^a\phi_{(-5)a} + M_5\phi_{(5)}^a\phi_{(-3)a} + M_3\phi_{(3)}^a\phi_{(-1)a}, \end{aligned}$$

(10)

where $\phi_{(7)}^a$, $\phi_{(5)}^a$, $\phi_{(3)}^a$, $(a = 1, \ldots, N)$ are fundamental, $\phi_{(-5)a}$, $\phi_{(-3)a}$, and $\phi_{(-1)a}$ are antifundamental representations of $U(N)$ global symmetry, and X is a $U(N)$ singlet. The field $\phi_{(r)}$ has an R charge r. We have chosen the real parameters f, N_3, N_5, M_3, M_5, and M_7 to be positive.

As we have discussed, this model breaks supersymmetry at the vacuum $\phi_{(r)} = 0$ for all r leaving the flat direction parametrized by X. In addition to this local minimum, there is a runaway direction to the true supersymmetric vacuum, which is obtained from the vacuum conditions (4). It is given by
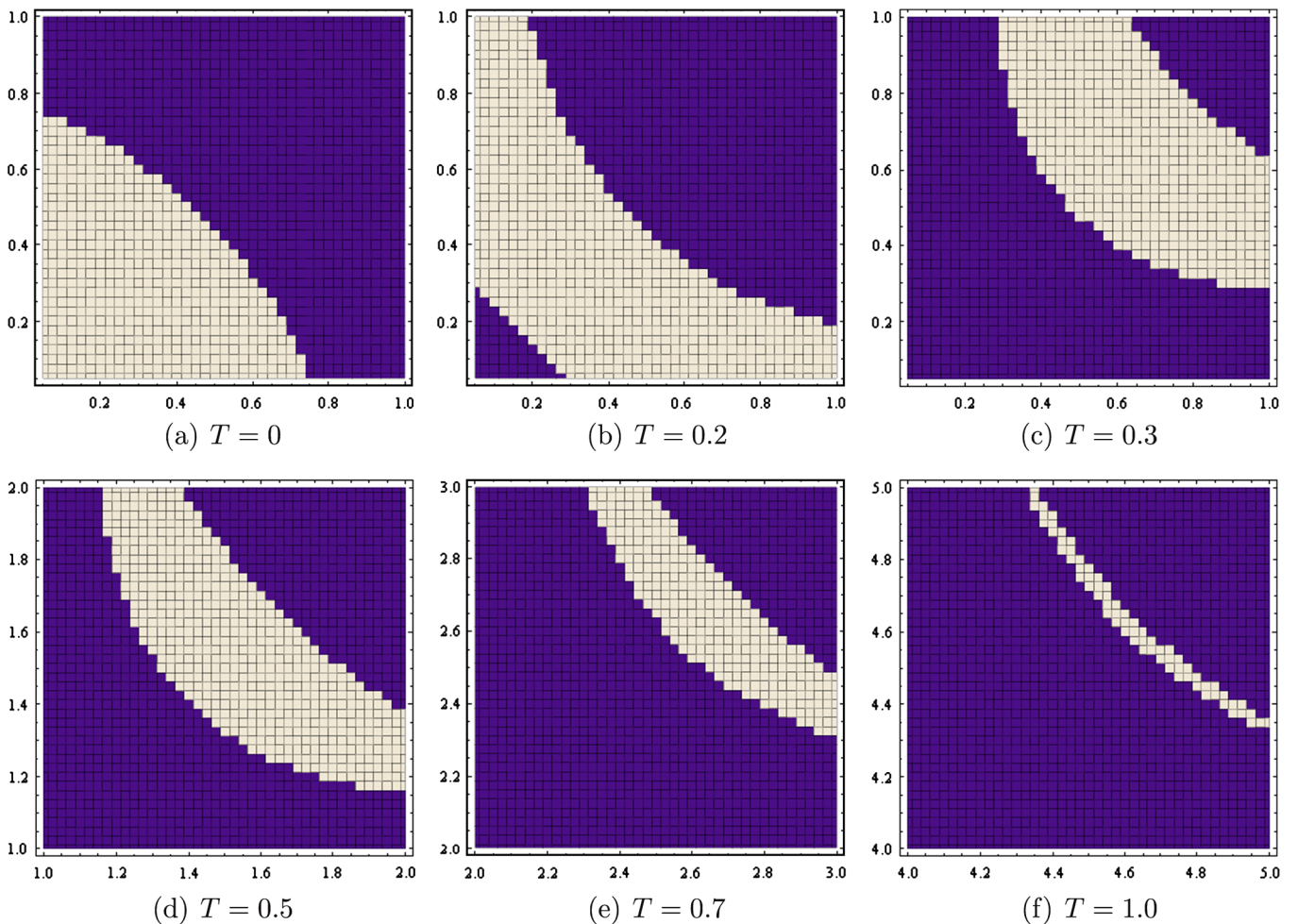

FIG. 1 (color online).   Contour plots of the allowed region of the $U(1)_R$ breaking against the parameters $(M_3/M_5, M_7/M_5)$ for $|X| < 3$ with temperatures ranging from $T = 0$ to 1.0. We choose values of the other parameters as $N_3 = N_5 = 1$, and $f/M_5^2 = 0.001$.

$$X = -\frac{M_5}{N_3}\frac{\phi_5}{\phi_3}\epsilon^{-2}, \qquad \phi_{(3)} = \epsilon\phi_3,$$

$$\phi_{(5)} = \epsilon^{-1}\phi_5, \qquad \phi_{(7)} = \frac{N_5 M_5}{N_3 M_7}\frac{\phi_5^2}{\phi_3}\epsilon^{-3},$$

$$\phi_{(-1)} = \frac{N_3 M_5}{N_5 M_3}\frac{\phi_{-3}^2}{\phi_{-5}}\epsilon^{-3}, \qquad \phi_{(-3)} = \epsilon^{-1}\phi_{-3},$$

$$\phi_{(-5)} = \epsilon\phi_{-5}, \tag{11}$$

where the constants f, N_3, N_5, ϕ_5, and ϕ_{-5} satisfy the following conditions:

$$f + 2N_5\phi_5\phi_{-5} = 0, \qquad N_3\phi_3\phi_{-3} = N_5\phi_5\phi_{-5}. \tag{12}$$

The runaway direction is characterized by a parameter $\epsilon \to 0$.

For later convenience, we rederive the result obtained in [6] for the allowed region of $U(1)_R$ breaking vacua in the parameter space of f, M, and N at zero temperature. Because the effective potential of the model with the $U(N)$ global symmetry is just the N copy of the one for the model with $N = 1$, it is enough to consider the $N = 1$ case to see the one-loop effective potential for X. We investigate the allowed regions for $(M_3/M_5, M_7/M_5)$ with $N_3 = N_5 = 1$ and $f/M_5^2 = 0.001$. The last value is chosen to satisfy the condition $|M^{-2}fN| \ll 1$ to avoid tachyonic directions for small X. The result is given in Fig. 1(a).

In the next section, we consider the one-loop effective potential at finite temperature and study the behavior of the parameter region that allows $U(1)_R$ breaking vacua. We will see how this parameter region changes according to nonzero temperature.

III. FINITE TEMPERATURE EFFECTS

The finite temperature contribution in the one-loop effective potential is given by [17]

$$V_B^{(1)}(\phi_c) = \frac{T^4}{2\pi^2}J_B[m_B^2(\phi_c)/T^2], \tag{13}$$

$$V_F^{(1)}(\phi_c) = -2\lambda\frac{T^4}{2\pi^2}J_F[m_F^2(\phi_c)/T^2], \tag{14}$$

where the first is real scalar and the second is fermionic contributions. Here T is temperature, ϕ_c are vacuum expectation values (VEVs) at vacua, and the fermionic degrees of freedom λ are given by $\lambda = 1$ (Weyl) or $\lambda = 2$

(Dirac). The functions J_B and J_F are the so-called bosonic and fermionic thermal functions given by

$$J_B[m^2\beta^2] = \int_0^\infty dx\, x^2 \log\left(1 - e^{-\sqrt{x^2 + \beta^2 m^2}}\right), \tag{15}$$

$$J_F[m^2\beta^2] = \int_0^\infty dx\, x^2 \log\left(1 + e^{-\sqrt{x^2 + \beta^2 m^2}}\right), \tag{16}$$

where $\beta = T^{-1}$. The one-loop effective potential is therefore given by

$$V_{\text{eff}} = V_{\text{tree}} + V_{\text{eff}}^{\text{CW}} + V_B^{(1)} + V_F^{(1)}. \tag{17}$$

In the following, we consider the effective potential (17) of the model (10). As discussed in the previous section, since the model has the $U(N)$ global symmetry, the effective potential (17) is just an N copy of the one with the $N = 1$ case. We therefore consider (17) with the $N = 1$ case. Since the high- and low-temperature expansions are useful to see the behavior of the potential analytically and to check the full numerical result, these expansions are collected in Appendix A.

For all the results in the following, the effective potential (17) is directly calculated by using the Coleman-Weinberg potential (8) and the thermal potentials (13) and (14) without any approximation formulas.

We show the parameter region which allows a nonsupersymmetric $U(1)_R$ breaking local minimum at temperatures ranging from $T = 0$ to $T = 1.0$ in Fig. 1. In this analysis, we study the allowed region against the parameters $(M_3/M_5, M_7/M_5)$ near the origin of X, $|X| \leq 3$. Their allowed region becomes smaller and the parameters $(M_3/M_5, M_7/M_5)$ have larger values, as temperature increases.

The numerical results in Fig. 1 enable us to see the structure of phase transitions of a given vacuum during the cooling process. It is seen that at high temperature the $U(1)_R$ symmetry is generically recovered, which is expected from the analytic calculations in Appendix A. As temperature decreases, with an appropriate choice of parameters, a vacuum that preserves the $U(1)_R$ symmetry at high temperature becomes a $U(1)_R$ breaking vacuum.

We note that the numerical result in Fig. 1 has a different behavior from the result of the model in [14], where the finite temperature effects of the same type of model as (1) without global symmetry have been studied. In [14], the contour plots similar to Fig. 1 are shown and it shows that once certain parameters come into an allowed region, they remain in the allowed region until zero temperature. However, in our model, some parameters entered into the
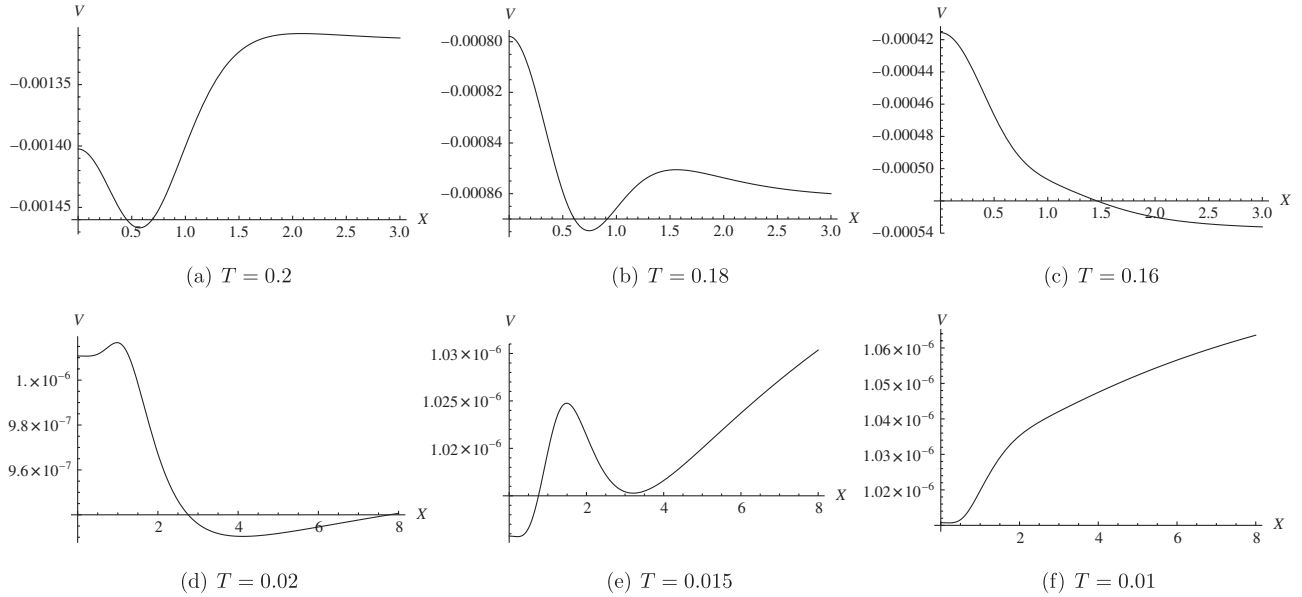
FIG. 2. Plots of potentials for X with temperatures ranging from $T = 0.2$ to $T = 0.01$. We choose $N_3 = N_5 = 1$, $M_3/M_5 = M_7/M_5 = 0.4$, and $f/M_5^2 = 0.001$. In the plots the numerical value is evaluated with $M_5 = 1$.

allowed region, then it goes out the region as temperature decreases. This fact means that there are several phase transitions during the cooling process. For instance, for the case with $N_3 = N_5 = 1$, $M_3/M_5 = M_7/M_5 = 0.4$, and $f/M_5^2 = 0.001$, the $U(1)_R$ symmetry vacuum takes place near the origin around $T \sim 0.25$ and it disappears around $T \sim 0.16$.

Eventually, this parameter choice realizes the $U(1)_R$ symmetry vacuum at zero temperature, but at lower temperatures, the evolution of vacuum structure is a bit nontrivial. Next, we will show detailed evolutions of the potential at lower temperature.

Figure 2 shows the plots of the potentials for X with $N_3 = N_5 = 1$, $M_3/M_5 = M_7/M_5 = 0.4$, and $f/M_5^2 = 0.001$. As we have discussed, there exists a $U(1)_R$ symmetry breaking vacuum near the origin for this parameter choice at the temperature around $T \sim 0.25$ and the vacuum disappears at a critical temperature as temperature decreases down to $T \sim 0.16$. This behavior can be seen in Figs. 2(a)–2(c). Although this $U(1)_R$ breaking vacuum around the origin disappeared at the critical temperature, the $U(1)_R$ breaking minimum reappears at lower temperatures. For instance, at $T = 0.16$ we find that there exists a $U(1)_R$ symmetry breaking vacuum around $X \sim 13$ which is far from the plot region of Fig. 2. As temperature decreases from $T = 0.16$, this vacuum approaches the origin as can be seen around $X \sim 4$ in Fig. 2(d). As temperature further decreases, the $U(1)_R$ symmetry breaking vacuum develops near the origin again [see Fig. 2(e)] because the Coleman-Weinberg potential becomes dominant and the extra vacuum far away from the origin disappears as can be seen in Fig. 2(f).

IV. RUNAWAY DIRECTION IN FINITE TEMPERATURE

In the previous section we studied the allowed region of the parameter space where $U(1)_R$ symmetry is broken. One would be afraid that thermal effects on the effective potential may prevent the state from staying in the vicinity of the metastable vacuum during the cooling process and the system may escape to the runaway vacuum through the ϕ directions. In this section we study finite temperature effects on a potential barrier that intermediates between the metastable vacuum and a runaway direction.

It is not easy to make a thorough investigation of how the structure of the effective potential, which depends not only on X but also $\phi_{(r)}$, is affected by the change of temperature. Instead, according to [10,14], we choose a particular path which passes from the metastable vacuum to a runaway direction and focus on the effective potential of the fixed path.

We choose a path, which is divided into two parts. The first part of the path includes the metastable vacuum while the other includes a runaway direction. The second path is chosen so that it is free of tachyonic modes. It is realized by imposing the condition $W^{ijk}W_k^\dagger = 0$ on the bosonic mass matrix (B1). In other words, it is the condition in which the bosonic mass matrix coincides with the fermionic one. Then the second part of the path sits on the surface determined by the relation $W^{ijk}W_k^\dagger = 0$, which is a two-dimensional subspace in the seven-dimensional space spanned by $\phi_{(5)}$, $\phi_{(-5)}$, $\phi_{(3)}$, $\phi_{(-3)}$, $\phi_{(7)}$, $\phi_{(-1)}$, and X. The first path is a straight line connecting the metastable vacuum and a point on the second path. The whole path is
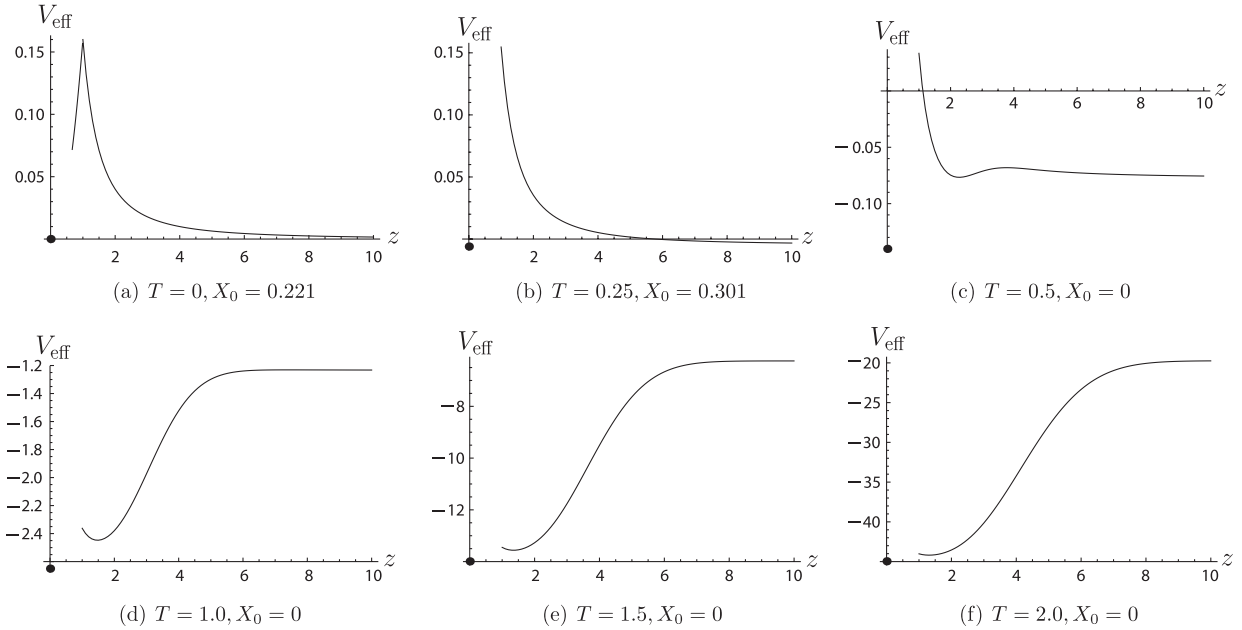
FIG. 3. The thermal effective potential on the path. The parameters are $M_3/M_5 = M_7/M_5 = 0.4$, $N_3 = N_5 = 1$, $f = 0.001$, and $\phi_3 = 1/M_5$. The black circles indicate the value of the origin ($z = 0$) at $X = X_0$, $\phi = 0$. In the interval $0 < z < 1$ the line is absent if tachyonic modes appear. In the plots the numerical value is evaluated with $M_5 = 1$.

parametrized by z. The metastable vacuum is at $z = 0$, and the runaway direction corresponds to $z \to \infty$.

The first part is given by

$$
\phi_{(5)} = -\frac{\phi_3 \hat{X}_0 N_3}{M_5} z, \qquad \phi_{(-5)} = \frac{f M_5}{2 N_3 N_5 \phi_3 \hat{X}_0} z,
$$

$$
\phi_{(3)} = \phi_3 z, \qquad \phi_{(-3)} = -\frac{f}{2 N_3 \phi_3} \zeta, \qquad (18)
$$

$$
\phi_{(7)} = \frac{N_3 N_5 \phi_3 \hat{X}_0^2}{M_5 M_7} z, \qquad \phi_{(-1)} = \frac{f \hat{X}_0}{2 M_3 \phi_3} z,
$$

$$
X = X_0(1 - \zeta) + \hat{X}_0 z \qquad (0 \le z \le 1).
$$

The second part of the path is given by

$$
\phi_{(5)} = -\frac{\phi_3 \hat{X}_0 N_3}{M_5} z, \qquad \phi_{(-5)} = \frac{f M_5}{2 N_3 N_5 \phi_3 \hat{X}_0} \frac{1}{z},
$$

$$
\phi_{(3)} = \frac{\phi_3}{z}, \qquad \phi_{(-3)} = -\frac{f}{2 N_3 \phi_3} z,
$$

$$
\phi_{(7)} = \frac{N_3 N_5 \phi_3 \hat{X}_0^2}{M_5 M_7} z^3, \qquad \phi_{(-1)} = \frac{f \hat{X}_0}{2 M_3 \phi_3} z^3, \qquad (19)
$$

$$
X = \hat{X}_0 z^2 \qquad (1 < z),
$$

where X_0 is the VEV of the metastable vacuum at the respective temperatures, and $\hat{X}_0 = X_0(T = 0)$. ϕ_3 is a constant.[2]

The effective potential on the path at various temperatures is shown in Fig. 3. The vanishing line indicates that tachyonic modes appear on the line (we call this the tachyonic line) and states cannot stay at that line. Therefore the state at the metastable vacuum keeps staying around the origin ($z = 0$) and never rolls down to the runaway vacuum.[3]

Since X is no longer (pseudo)modulus at states with nonzero VEVs for $\phi_{(r)}$, the mass matrices (6) and (7) are not available to derive the effective potential. The comprehensive mass matrices M_B and M_F are given in Appendix B. The above condition $W^{ijk} W_k^\dagger = 0$ leads to

$$
\phi_{(5)} = -\frac{N_3 \phi_{(3)} X}{M_5}, \qquad \phi_{(-5)} = \frac{f M_5}{2 N_3 N_5 \phi_{(3)} X},
$$

$$
\phi_{(-3)} = -\frac{f}{2 N_3 \phi_{(3)}}, \qquad \phi_{(7)} = \frac{N_3 N_5 \phi_{(3)} X^2}{M_5 M_7}, \qquad (20)
$$

$$
\phi_{(-1)} = \frac{f X}{2 M_3 \phi_{(3)}}.
$$

All VEVs in the mass matrices can be taken to be real by field redefinitions without loss of generality. One can show that (20) are equivalent to (11) and (12) by replacing

---

[2]We choose a simply connected path rather than a smoothly connected path such as in [14], because even small perturbation around (20) makes tachyonic modes in the practical calculation.

[3]The absolute value of the effective potential at the origin is different from that in Fig. 2, since the size of the mass matrices increased by 2. Because of the finite temperature effect, even a massless field contributes to the effective potential. This contribution is the constant given by $-\frac{T^4}{2\pi^2}(\frac{\pi^4}{45} + \frac{7\pi^4}{360}) \times 2 \approx -0.41 T^4$.

$\phi_{(3)} \rightarrow \epsilon\phi_3$ and $\phi_{(5)} \rightarrow \epsilon^{-1}\phi_5$. In fact the tree-level potential on the surface (20) is written as

$$V_{\text{tree}} = \frac{f^2 M_5^2 M_7^2}{4N_3^2 N_5^2 |\phi_{(3)}|^2 |X|^2} + M_3^2 |\phi_{(3)}|^2. \quad (21)$$

Taking a limit of $\phi_{(3)} \rightarrow 0$, $X \rightarrow \infty$, and $X\phi_{(3)} \rightarrow \infty$ at the same time, V_{tree} goes to a supersymmetric global vacuum.

The qualitative behavior of the effective potential in Fig. 3 is confirmed by an analytic calculation without any specification of parameters. At high temperature, the expansion (A3) can be applied. The effective potential on the surface (19) becomes

$$V_{\text{eff}} = V_{\text{tree}} - \frac{7}{24}\pi^2 T^4 + \frac{T^2}{16}\Big\{4\hat{X}_0^2(N_3^2 + N_5^2)z^4$$
$$+ \Big(\frac{f^2}{\phi_3^2} + \frac{4\hat{X}_0^2\phi_3^2 N_3^2 N_5^2}{M_5^2}\Big)z^2 + \mathcal{O}(z^0)\Big\}$$
$$+ \frac{T}{2\pi}(f\hat{X}_0(N_3^2 + N_5^2)z^2 + \mathcal{O}(z^{-2})) + \cdots, \quad (22)$$

where the Coleman-Weinberg potential is absent as mentioned before. One can see that V_{eff} increases as $\sim z^4$ for $z \gtrsim 1$, and thus the potential is always minimized at $z = 1$ on the second part of the path. This suggests that, at high temperature, the stable state exists at least in the region $z \lesssim 1$.

We summarize the evolution of the vacuum structure on the path for the choice of parameters, $N_3 = N_5 = 1$, $M_3/M_5 = M_7/M_5 = 0.4$, and $f/M_5^2 = 0.001$ which is considered throughout this paper. These parameters allow a vacuum with $U(1)_R$ symmetry breaking at zero temperature. At high temperature supersymmetry breaking vacuum sits at the origin of the field space (X, z) where $U(1)_R$ symmetry is not broken. As the temperature decreases, a potential barrier between the origin and the z direction develops and a local vacuum appears along the z direction (Fig. 3), which has a higher potential value than the one at the origin. So the origin remains favored as a vacuum.

There is a local vacuum along the z direction at certain temperatures $T = 0.5$–2.0 which is separated from the metastable vacuum by the tachyonic line as we have mentioned. Meanwhile, the supersymmetric runaway vacuum develops along the $z \rightarrow \infty$ direction around $T = 0.5$. Although the runaway vacuum may be energetically favored compared to the metastable vacuum, the local minimum at the origin remains a vacuum state due to the large potential barrier between the origin and the runaway vacuum.

Simultaneously, the local vacuum at the origin of ϕ directions ($z = 0$) starts to roll down to a local vacuum near the origin along the X direction where the $U(1)_R$ symmetry is broken. The large potential barrier between the X direction and the ϕ directions prevents the $U(1)_R$

breaking vacuum from decaying to the runaway vacuum and keeps it sitting on the metastable vacuum.

V. CONCLUSIONS AND DISCUSSIONS

We have studied finite temperature effects on O'Raifeartaigh-type models with $U(N)$ global symmetry where supersymmetry is spontaneously broken. At zero temperature the model has a metastable vacuum where $U(1)_R$ symmetry is dynamically broken by the one-loop corrections for appropriate parameter regions. In addition to a metastable vacuum there also exists a runaway vacuum. We have investigated the finite temperature effects in the effective potential of the pseudomodulus field X. In order to consider the finite temperature effects along the runaway direction, we chose a particular path so that tachyonic modes can be avoided.

The main features of our study are summarized as follows:

(i) Even though we have taken $N = 1$ to study the effective potential, the finite temperature effects for the superpotential (10) that allows the global symmetry $U(N)$ is nontrivial. The phase structure during the cooling process is highly dependent on the parameter matrices M^{ij} and N^{ij}. These matrices cannot be chosen freely once one imposes the global symmetries. As we have mentioned in the Introduction, the global symmetry is a key point when one considers the mediation of supersymmetry breaking.

(ii) Our study reveals the effect of the intermediate and low-temperature region particularly. Many of the preceding analyses do not pay much attention to that region; however, when one considers the cooling of the universe, it requires rigorous information in the intermediate and low-temperature region as well as high temperature. As anticipated from the analytic calculations, the $U(1)_R$ symmetry is recovered at high temperature which is the similar result found in the O'Raifeartaigh model without global symmetries [14]. However, we find nontrivial vacuum structures—the landscape—at low temperatures. Certain parameter regions that do not have the meta-stable vacua at zero temperature can possess $U(1)_R$ breaking metastable vacuum at finite (low) temperature. This structure is not seen in the O'Raifeartaigh model without global symmetries [14]. We obtained this result by performing the full numerical analysis without any (high- and low-temperature) approximations.

(iii) To obtain the correct value of the effective potential in the runaway direction, we introduce an inherently tachyon-free path where the bosonic mass matrix coincides with the fermionic one. Another possible way of the path that is used in [14] is a smooth connection between the metastable and a runaway vacuum at zero temperature with

weighting function. That kind of path is not appropriate for our case as pointed out in Sec. IV, since in the practical calculation it makes tachyonic modes on the path and causes meaningless analyses. The choice of the path is critical.

We make some comments about a previous study. In the literature [15], the thermal effective potential of a class of the O'Raifeartaigh model which includes the model of the present paper has been analyzed. The author concludes that within a certain high-temperature region a new metastable vacuum that is absent at zero temperature is developed far away from the origin $X = 0$. This kind of vacuum is not considered in Sec. IV. The main reason for this is the difference of the focusing point and analysis. In [15], the massive scalar fields ϕ are integrated out to analyze the runaway behavior $X \to \infty$, before introducing thermal effects. Then the thermal potential is given in analytic form by using a high-temperature expansion formula. Meanwhile, we keep all the fields explicitly, make the complete mass matrices, calculate eigenvalues of the mass matrices, and focus on the effective potential along the fixed path, particularly not far from the origin of ϕ and X, by using numerical calculation.

We close this work by pointing out future directions. Here we studied the hidden sector that the $U(1)_R$ symmetry breaking is spontaneously broken by the one-loop corrections in $\mathcal{N} = 1$ supersymmetric theory. However, in some $\mathcal{N} = 1$ supersymmetric models, especially accompanying strong gauge dynamics, the perturbative treatment is not available for all regions of the pseudoflat direction. For instance, in the Izawa-Yanagida-Intriligator-Thomas model [18,19], where an O'Raifeartaigh-type sector is dynamically generated by strong gauge dynamics in the low-energy superpotential, in order to remove the degeneracy of the pseudomoduli, we have to take account of quantum corrections for the Kähler potential. In general, this is a very difficult task since the Kähler potential is not holomorphic and thus quantum corrections can be estimated at best by perturbative means only in the ultraviolet (weak coupling) region of the moduli space parametrizing the pseudoflat direction which is far from the origin. Therefore, the potential behavior in the infrared region remains unclear. However, in an $\mathcal{N} = 2$ supersymmetric gauge theory one can derive the exact low-energy effective action as demonstrated by Seiberg and Witten [20,21], using the properties of holomorphy and duality. In the framework of $\mathcal{N} = 2$ supersymmetric gauge theory, some supersymmetry breaking models with $U(1)_R$ symmetry breaking were considered [22–26]. It would be interesting to study effects of the finite temperature in those models (see also [27]).

APPENDIX A: EFFECTIVE POTENTIAL AT HIGH AND LOW TEMPERATURES

1. High-temperature expansion

In this section, we consider series expansions of the thermal functions at high temperature. For $m/T \ll 1$, we have the following expansions:

$$J_B[m^2/T^2] = -\frac{\pi^4}{45} + \frac{\pi^2}{12}\frac{m^2}{T^2} - \frac{\pi}{6}\frac{m^3}{T^3} - \frac{1}{32}\frac{m^4}{T^4}$$
$$\times \log\frac{m^2}{a_b T^2} - 2\pi^{7/2}\sum_{l=1}^{\infty}(-1)^l\frac{\zeta(2l+1)}{(l+1)!}$$
$$\times \Gamma\left(l+\frac{1}{2}\right)\left(\frac{m^2}{4\pi^2 T^2}\right)^{l+2}, \tag{A1}$$

and

$$J_F[m^2/T^2] = \frac{7\pi^4}{360} - \frac{\pi^2}{24}\frac{m^2}{T^2} - \frac{1}{32}\frac{m^4}{T^4}\log\frac{m^2}{a_f T^2}$$
$$- \frac{\pi^{7/2}}{4}\sum_{l=1}^{\infty}(-1)^l\frac{\zeta(2l+1)}{(l+1)!}(1-2^{-2l-1})$$
$$\times \Gamma\left(l+\frac{1}{2}\right)\left(\frac{m^2}{\pi^2 T^2}\right)^{l+2}, \tag{A2}$$

where ζ is the Riemann zeta function, $a_b = 16\pi^2\exp(3/2 - 2\gamma_E)$, $a_f = \pi^2\exp(3/2 - 2\gamma_E)$, and $\gamma_E \sim 0.577$ is the Euler-Mascheroni constant. Therefore the finite temperature part of the effective potential (17) is given by

$$V^{(1)}(\phi_c, T) = -\frac{\pi^2 T^4}{90}\left(N_s + \lambda\frac{7}{4}N_F\right) + \frac{T^2}{24}\left[\sum_i^{N_s} m_B^2(\phi_c)_i\right.$$
$$\left. + \sum_i^{N_F}\lambda m_F^2(\phi_c)_i\right] - \frac{T}{12\pi}\sum_i^{N_s} m_B^3(\phi_c)_i + \cdots, \tag{A3}$$

where the dots denote terms that are subleading in m/T. N_s, N_F are the number of real scalars and Weyl fermions and m_{Bi}, m_{Fi} are mass eigenvalues of the boson and fermion mass matrices.

In general, it is hard to find the mass eigenvalues analytically. However, one can extract high-temperature effects without solving eigenvalue equations explicitly. At very high temperature $T/m \gg 1$, the $\mathcal{O}(T^2)$ term is dominant compared to the $\mathcal{O}(T)$ terms in (A3),[4] the coefficient of T^2

---

[4]In (A3), the $\mathcal{O}(T^4)$ term is just the numerical constant and is irrelevant for analyzing the X dependence.

in $V^{(1)}$ is given by the trace of mass matrices m_B^2 and m_F^2. In our model we find

$$\sum_i m_{Bi}^2 + \sum_i m_{Fi}^2 = 8(M_3^2 + M_5^2 + M_7^2 + N_3^2 X^2 + N_5^2 X^2), \tag{A4}$$

where we have chosen all the parameters real for simplicity. From the expression of the mass matrices, it is easy to see that the result is independent of the parameter f. The effective potential behaves as

$$V^{(1)}(X, T) \sim T^2(N_3^2 + N_5^2)X^2 + \mathcal{O}(T). \tag{A5}$$

From this expression, one sees that the modulus X tends to be fixed at the origin at high temperature if N_3 and N_5 are not zero. Therefore, we expect that the region that allows $U(1)_R$ breaking vacua is becoming small at high temperature. In fact, this behavior can be observed in numerical analysis of the full effective potential (17) (see Fig. 1).

2. Low-temperature expansion

Let us derive an expression that is useful to study the behavior of the effective potential at low temperature. For the case $m/T \gg 1$, the bosonic thermal function is expanded as

$$J_B = \int_0^\infty ds\, s^2 \sum_{n=1}^\infty (-1)\frac{X^n(s)}{n}, \tag{A6}$$

where $X(s) \equiv e^{-\sqrt{s^2 + m^2\beta^2}}$. The integral over s is rewritten by defining the new variable $s = m\beta \sinh t$ as

$$J_B = \int_0^\infty dt \sum_{n=1}^\infty \frac{1}{n}\left(\frac{m^3}{n^3}\frac{d^3}{dm^3} - \frac{m^3\beta^2}{n}\frac{d}{dm}\right)e^{-nm\beta\cosh t}. \tag{A7}$$

This integration is expressed by the modified Bessel functions:

$$J_B = \frac{m^3\beta^3}{4}\sum_{n=1}^\infty \frac{1}{n}(K_1(nm\beta) - K_3(nm\beta)), \tag{A8}$$

where we have used the expression $K_0(z) = \int_0^\infty dt\, e^{-z\cosh t}$ and relations

$$\frac{d}{dz}K_0(z) = -K_1(z),$$
$$\frac{d^3}{dz^3}K_0(z) = -\frac{3}{4}K_1(z) - \frac{1}{4}K_3(z). \tag{A9}$$

Similarly, we have the fermionic thermal function as

$$J_F = \frac{m^3\beta^3}{4}\sum_{n=1}^\infty \frac{1}{n}(-1)^n(K_1(nm\beta) - K_3(nm\beta)). \tag{A10}$$

Let us use the asymptotic expansion of the modified Bessel functions

$$K_\nu(z) \sim \sqrt{\frac{\pi}{2}}\frac{1}{\sqrt{z}}e^{-z}\sum_{l=0}^\infty \frac{1}{(2z)^l}\frac{\Gamma(\nu + l + 1/2)}{l!\Gamma(\nu - l + 1/2)}$$
$$= \sqrt{\frac{\pi}{2}}\frac{1}{\sqrt{z}}e^{-z}\left(1 + \frac{4\nu^2 - 1}{8z} + \cdots\right) \quad (|z| \to \infty), \tag{A11}$$

where the dots are subleading order in z^{-l}. Then, we have

$$J_B(m\beta) \sim -\sqrt{\frac{\pi}{2}}(m\beta)^{3/2}\mathrm{Li}_{5/2}(e^{-m\beta}). \tag{A12}$$

Here $\mathrm{Li}_s(z) = \sum_{k=1}^\infty \frac{z^k}{k^s}$ is the polylogarism function and we have used the fact that the dominant contribution comes from the $n = 1$ sector in the expansions (A8) and (A10). Again, using the asymptotic behavior $\mathrm{Li}_s(z) = z + 2^{-s}z^2 + 3^{-s}z^3 + \cdots (|z| \to 0)$, we find the low-temperature expansion of the thermal functions

$$J_B(m\beta) \sim -\sqrt{\frac{\pi}{2}}(m\beta)^{3/2}(e^{-m\beta} + 2^{-5/2}e^{-2m\beta}$$
$$+ 3^{-5/2}e^{-3m\beta} + \cdots), \tag{A13}$$

$$J_F(m\beta) \sim -\sqrt{\frac{\pi}{2}}(m\beta)^{3/2}(-e^{-m\beta} + 2^{-5/2}e^{-2m\beta}$$
$$- 3^{-5/2}e^{-3m\beta} + \cdots). \tag{A14}$$

As we have discussed, at the origin of ϕ^i, the mass for ϕ^i is given by $m \sim M + NX$. Therefore we expect that the finite temperature part of the effective potential at low temperature behaves similar to

$$V^{(1)}(X, T) \sim -T^4\mathrm{Tr}\{((M + NX)T^{-1})^{3/2}e^{-(M+NX)T^{-1}}\}. \tag{A15}$$

This expression would be useful for a calculable model to see the thermal evolution of vacuum analytically at low temperature. In our case, since analytic forms of eigenvalues are complicated, it is difficult to see the evolution analytically. However, the low-temperature expansion is still useful for numerical calculations. It needs shorter time to evaluate the effective potential compared to the full thermal functions (15) and (16). One can use the low-temperature expansion to check the full result in the numerical analysis in Sec. III.

APPENDIX B. MASS MATRICES

The general mass matrices are given as follows:

$$M_B^2 = \begin{pmatrix} W_{ik}^\dagger W^{kj} & W_{ijk}^\dagger W^k \\ W^{ijk}W_k^\dagger & W^{ik}W_{kj}^\dagger \end{pmatrix}, \tag{B1}$$

$$M_F^2 = \begin{pmatrix} W_{ik}^\dagger W^{kj} & 0 \\ 0 & W^{ik}W_{kj}^\dagger \end{pmatrix}, \tag{B2}$$

where

$$W_{ik}^\dagger W^{kj} = (W^{ik} W_{kj}^\dagger)^\dagger$$

$$
= \begin{pmatrix}
M_5^2 + N_5^2(|X|^2 + |\phi_{-5}|^2) & N_5^2 \phi_5 \phi_{-5}^\dagger & N_3(M_5 X + N_5 \phi_{-3}\phi_{-5}^\dagger) & N_3 N_5 \phi_3 \phi_{-5}^\dagger & M_7 N_5 X^\dagger & 0 & M_5 N_3 \phi_3 + N_5^2 X^\dagger \phi_5 \\
N_5^2 \phi_{-5}\phi_5^\dagger & M_7^2 + N_5^2(|X|^2 + |\phi_5|^2) & N_3 N_5 \phi_{-3}\phi_5^\dagger & N_5(M_5 X^\dagger + N_3 \phi_3 \phi_5^\dagger) & 0 & 0 & N_5^2 \phi_{-5} X^\dagger \\
N_3(M_5 X^\dagger + N_5 \phi_{-5}\phi_{-3}^\dagger) & N_3 N_5 \phi_5 \phi_{-3}^\dagger & M_3^2 + N_3^2(|X|^2 + |\phi_{-3}|^2) & N_3^2 \phi_3 \phi_{-3}^\dagger & 0 & 0 & N_3^2 X^\dagger \phi_3 \\
N_3 N_5 \phi_{-5}\phi_3^\dagger & N_5(M_5 X + N_3 \phi_5 \phi_3^\dagger) & N_3^2 \phi_{-3}\phi_3^\dagger & M_5^2 + N_3^2(|X|^2 + |\phi_3|^2) & 0 & M_3 N_3 X^\dagger & M_5 N_5 \phi_{-5} + N_3^2 X^\dagger \phi_{-3} \\
M_7 N_5 X & 0 & 0 & 0 & M_7^2 & 0 & M_7 N_5 \phi_5 \\
0 & 0 & 0 & M_3 N_3 X & 0 & M_3^2 & M_3 N_3 \phi_{-3} \\
M_5 N_3 \phi_3^\dagger + N_5^2 X \phi_5^\dagger & N_5^2 X \phi_{-5}^\dagger & N_3^2 X \phi_3^\dagger & M_5 N_5 \phi_{-5}^\dagger + N_3^2 X \phi_{-3}^\dagger & M_7 N_5 \phi_5^\dagger & M_3 N_3 \phi_{-3}^\dagger & N_5^2(|\phi_3|^2 + |\phi_5|^2 + |\phi_{-3}|^2 + |\phi_{-5}|^2)
\end{pmatrix},
$$

(B3)

$$W_{ijk}^\dagger W^k = (W^{ijk} W_k^\dagger)^\dagger$$

$$
= \begin{pmatrix}
0 & N_5(f + N_3 \phi_3 \phi_{-3} + N_5 \phi_5 \phi_{-5}) & 0 & 0 & 0 & 0 & N_5(N_5 X \phi_5 + M_7 \phi_7) \\
N_5(f + N_3 \phi_3 \phi_{-3} + N_5 \phi_5 \phi_{-5}) & 0 & 0 & 0 & 0 & 0 & N_5(N_5 X \phi_{-5} + M_5 \phi_{-3}) \\
0 & 0 & 0 & N_3(f + N_3 \phi_3 \phi_{-3} + N_5 \phi_5 \phi_{-5}) & 0 & 0 & N_3(N_3 X \phi_3 + M_5 \phi_5) \\
0 & 0 & N_3(f + N_3 \phi_3 \phi_{-3} + N_5 \phi_5 \phi_{-5}) & 0 & 0 & 0 & N_3(N_3 X \phi_{-3} + M_3 \phi_{-1}) \\
0 & 0 & 0 & 0 & 0 & 0 & 0 \\
0 & 0 & 0 & 0 & 0 & 0 & 0 \\
N_5(N_5 X \phi_5 + M_7 \phi_7) & N_5(N_5 X \phi_{-5} + M_5 \phi_{-3}) & N_3(N_3 X \phi_3 + M_5 \phi_5) & N_3(N_3 X \phi_{-3} + M_3 \phi_{-1}) & 0 & 0 & 0
\end{pmatrix}.
$$

(B4)

X and ϕ_r are VEVs of X and $\phi_{(r)}$, respectively.

[1] A. E. Nelson and N. Seiberg, Nucl. Phys. **B416**, 46 (1994).
[2] K. A. Intriligator, N. Seiberg, and D. Shih, J. High Energy Phys. 04 (2006) 021.
[3] L. O'Raifeartaigh, Nucl. Phys. **B96**, 331 (1975).
[4] D. Shih, J. High Energy Phys. 02 (2008) 091.
[5] Z. Komargodski and D. Shih, J. High Energy Phys. 04 (2009) 093.
[6] L. Ferretti, J. High Energy Phys. 12 (2007) 064.
[7] M. Dine and J. Mason, Phys. Rev. D **77**, 016005 (2008); R. Kitano, H. Ooguri, and Y. Ookouchi, Phys. Rev. D **75**, 045022 (2007); C. Csaki, Y. Shirman, and J. Terning, J. High Energy Phys. 05 (2007) 099; S. Abel, C. Durnford, J. Jaeckel, and V. V. Khoze, Phys. Lett. B **661**, 201 (2008); N. Haba and N. Maru, Phys. Rev. D **76**, 115019 (2007); B. K. Zur, L. Mazzucato, and Y. Oz, J. High Energy Phys. 10 (2008) 099; S. Abel, J. Jaeckel, V. V. Khoze, and L. Matos, J. High Energy Phys. 03 (2009) 017; R. Essig, J. F. Fortin, K. Sinha, G. Torroba, and M. J. Strassler, J. High Energy Phys. 03 (2009) 043; S. A. Abel, J. Jaeckel, and V. V. Khoze, Phys. Lett. B **682**, 441 (2010); N. Craig, R. Essig, S. Franco, S. Kachru, and G. Torroba, Phys. Rev. D **81**, 075015 (2010); T. T. Yanagida and K. Yonekura, Phys. Rev. D **81**, 125017 (2010).
[8] H. Murayama and Y. Nomura, Phys. Rev. Lett. **98**, 151803 (2007); O. Aharony and N. Seiberg, J. High Energy Phys. 02 (2007) 054; H. Murayama and Y. Nomura, Phys. Rev. D **75**, 095011 (2007); H. Y. Cho and J. C. Park, J. High Energy Phys. 09 (2007) 122; S. Franco and S. Kachru, Phys. Rev. D **81**, 095020 (2010); S. Schafer-Nameki, C. Tamarit, and G. Torroba, J. High Energy Phys. 03 (**2011**) 113; S. R. Behbahani, N. Craig, and G. Torroba, Phys. Rev. D **83**, 015004 (2011); L. G. Aldrovandi and D. Marques, J. High Energy Phys. 05 (2008) 022; D. Marques and F. A. Schaposnik, J. High Energy Phys. 11 (2008) 077.
[9] S. Kachru, R. Kallosh, A. D. Linde, and S. P. Trivedi, Phys. Rev. D **68**, 046005 (2003).
[10] S. A. Abel, C. S. Chu, J. Jaeckel, and V. V. Khoze, J. High Energy Phys. 01 (2007) 089.
[11] N. J. Craig, P. J. Fox, and J. G. Wacker, Phys. Rev. D **75**, 085006 (2007).
[12] W. Fischler, V. Kaplunovsky, C. Krishnan, L. Mannelli, and M. A. C. Torres, J. High Energy Phys. 03 (2007) 107.
[13] S. A. Abel, J. Jaeckel, and V. V. Khoze, J. High Energy Phys. 01 (2007) 015.
[14] E. F. Moreno and F. A. Schaposnik, J. High Energy Phys. 10 (2009) 007.
[15] A. Katz, J. High Energy Phys. 10 (2009) 054.
[16] S. R. Coleman and E. J. Weinberg, Phys. Rev. D **7**, 1888 (1973).
[17] L. Dolan and R. Jackiw, Phys. Rev. D **9**, 3320 (1974).
[18] K. I. Izawa and T. Yanagida, Prog. Theor. Phys. **95**, 829 (1996).
[19] K. A. Intriligator and S. D. Thomas, Nucl. Phys. **B473**, 121 (1996).
[20] N. Seiberg and E. Witten, Nucl. Phys. **B426**, 19 (1994); **B430**, 485(E) (1994).

[21] N. Seiberg and E. Witten, Nucl. Phys. **B431**, 484 (1994).

[22] M. Arai and N. Okada, Phys. Rev. D **64**, 025024 (2001); Nucl. Phys. B, Proc. Suppl. **102–103**, 219 (2001).

[23] M. Arai, C. Montonen, N. Okada, and S. Sasaki, Phys. Rev. D **76**, 125009 (2007).

[24] H. Ooguri, Y. Ookouchi, and C. S. Park, Adv. Theor. Math. Phys. **12**, 405 (2008).

[25] G. Pastras, arXiv:0705.0505.

[26] J. Marsano, H. Ooguri, Y. Ookouchi, and C. S. Park, Nucl. Phys. **B798**, 17 (2008).

[27] E. Katifori and G. Pastras, arXiv:0811.3393.